3-D Modeling of Surface-Acoustic-Wave Based Sensor

Yeswanth L Rao and Guigen Zhang
Micro/Nano Bioengineering Laboratory
University of Georgia
COMSOL Users Conference, Newton, MA, Oct. 4-6, 2007

Outline

- Background on SAW sensors
- Research questions & objectives
- Modeling approach
- Results and discussion
- Conclusions

General Requirements of a Sensor

- High sensitivity
- High selectivity
- Good response time
- Wireless capability
- Real time and in-situ measurements
- Reproducible response

Why SAW Devices?

- Operates at a high frequency (MHz-GHz) - high resolution, high sensitivity
- Room temperature operation
- Can work on a wireless platform
- Can work in both dry and aqueous environments (eg: gas sensors, biosensors)
- Simple fabrication techniques

Principle of Operation of a SAW Sensor

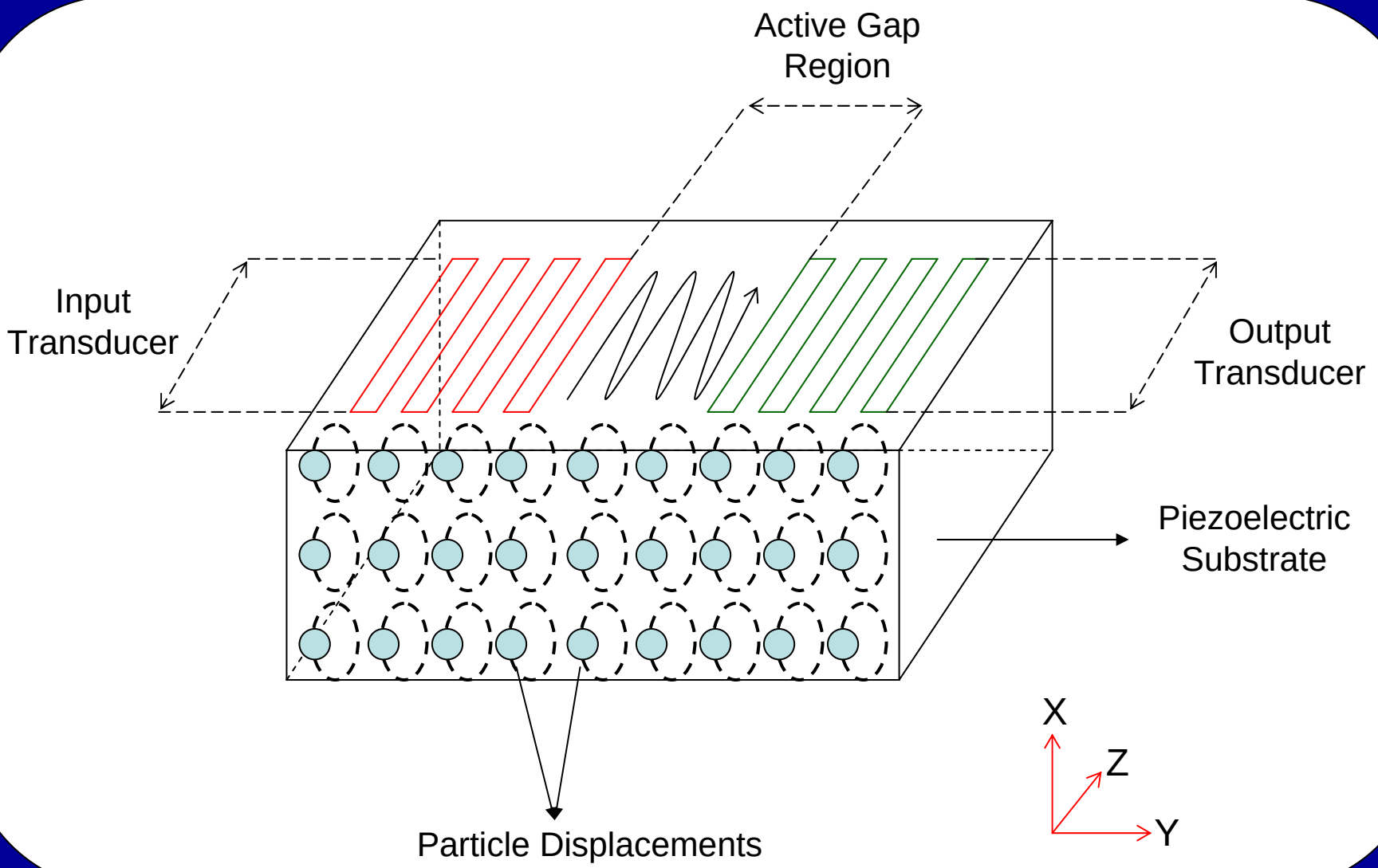

Principle of Operation of a SAW Sensor

- **Mass loading in the active area will lead to signal attenuation and frequency shift**
- **It is hypothesized that nanostructures in the active gap region will provide increased surface area for mass loading thereby increasing the sensitivity of the sensor.**

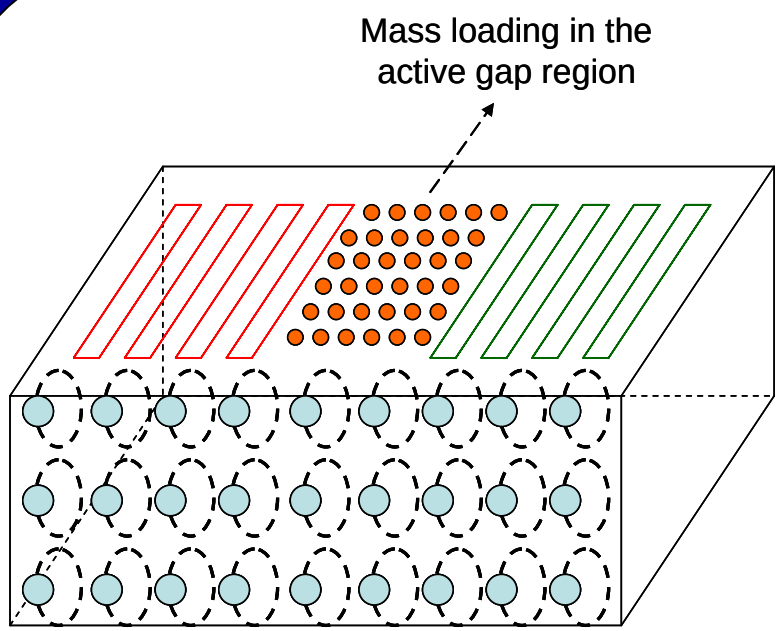

Mass loading in the active gap region
without nanostructures

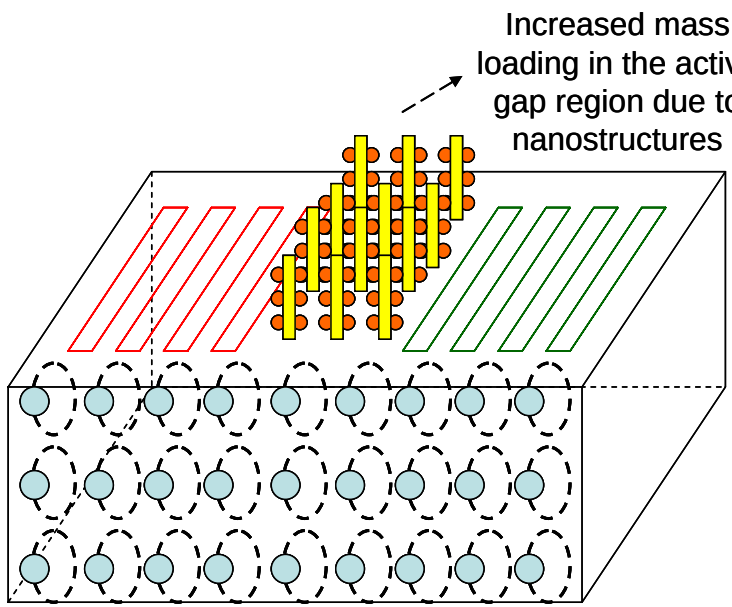

Mass loading in the active gap region
with nanostructures

Research Questions & Objectives

Questions

- **Can the detection sensitivity be increased by integrating nanostructures on a SAW sensor?**
- **How will these nanostructures affect the wave propagation characteristics?**
- **Will the sensitivity increase by using a piezoceramic material as the sensing layer instead of the conventional metallic layer?**

Objectives

- **To develop a full scale 3-D computational model to understand the SAW wave propagation characteristics in order to help build a SAW sensor with enhanced sensitivity.**

Model Development

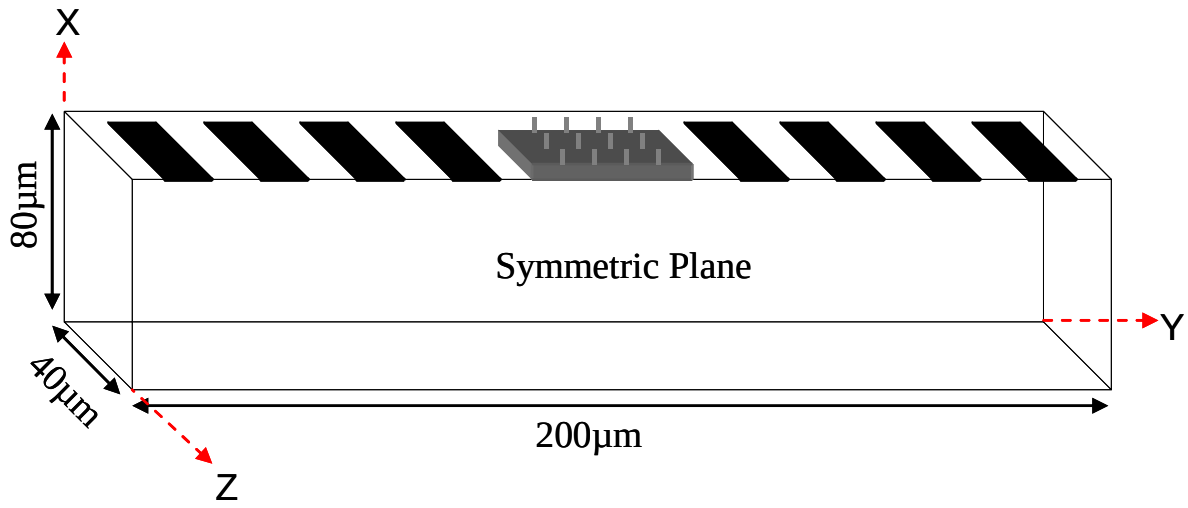

Schematic representation of the SAW sensor

- **XY Lithium Niobate (200µm x 80µm x 40 µm) is the piezoelectric substrate where Y is the wave propagation direction.**
- **Interdigitated transducers (10 µm width x 10 µm spacing) are treated as massless conductive boundaries.**
- **Gold square nanopillars (100nm width x 1µm height) are placed on top of the gold active layer (20µm x 20µm x 1 µm).**
- **Sensor performance is evaluated before and after 100nm PMMA adsorption (represents anylate adsorption).**

Modeling Approach

- **To investigate the effect of nanostructures on SAW propagation, the following models were developed**
  - **SAW delay line with gold active layer**
  - **SAW delay line with gold active layer along with 9 nanopillars**
  - **SAW delay line with gold active layer along with 12 nanopillars**
- **To investigate the effect of replacing the conventional active layer with a piezo material, the following models were developed**
  - **SAW delay line with gold active layer**
  - **SAW delay line with lithium nioabate active layer**

Modeling Approach

- **Input – Two types of wave perturbation was used:**
  - **Impulse wave function**

$$V_{i+} = \begin{cases} +0.5V, t \le 1ns \\ 0V, t > 1ns \end{cases}, V_{i-} = \begin{cases} -0.5V, t \le 1ns \\ 0V, t > 1ns \end{cases}$$

where V_{i+} and V_{i-} were applied to the alternate fingers of the generator IDT

  - **Sinusoidal wave function**

$$V_i = 1 \times \sin(2\pi \times f \times t),\ f = 100MHz, t = 100ns$$

where V_i is applied to the alternate fingers of the generator IDT while the others are grounded

- **Output – voltage at the alternate fingers of the receiver IDT is measured and the insertion loss is calculated by taking the ratio of output signal to input**

$$IL = 20 \times \log_{10} \left| v_{output} / v_{input} \right| (dB)$$

- **Sensitivity – The differential signal attenuation per unit mass loading is determined as a measure of detection sensitivity**

Governing Equations

- **Acoustic wave propagation is governed by Gauss law for its electrical behavior and Newton's law for its mechanical behavior.**

$$T = C^E \bullet S - e \bullet E \qquad D = e \bullet S + \varepsilon^s \bullet E$$

$$\nabla \bullet [e \bullet \nabla \varphi] + \nabla \bullet [C^E \bullet \nabla_s u] - \rho \ddot{u} = 0 \qquad \nabla \bullet [e \bullet \nabla_s u] = \nabla \bullet [\varepsilon^s \bullet (\nabla \varphi)]$$

Where T is the stress tensor, C_E the elasticity matrix, S the strain tensor, e the piezoelectric coupling matrix, E the electric field vector, D the electrical displacement, ε^s the permittivity matrix, φ the electrical potential, ü is the particle displacement and the particle acceleration.

- **The elasticity matrix, stress matrix and relative permittivity matrix for the XY lithium niobate substrate can be expressed as:**

$$C = \begin{pmatrix} C_{11} & C_{12} & C_{13} & C_{14} & 0 & 0 \\ C_{12} & C_{11} & C_{13} & -C_{14} & 0 & 0 \\ C_{13} & C_{13} & C_{33} & 0 & 0 & 0 \\ C_{14} & -C_{14} & 0 & C_{44} & 0 & 0 \\ 0 & 0 & 0 & 0 & C_{44} & C_{14} \\ 0 & 0 & 0 & 0 & C_{14} & (C_{11}-C_{12})/2 \end{pmatrix}$$

Elasticity Matrix

$$e = \begin{pmatrix} 0 & 0 & 0 & 0 & e_{15} & -e_{22} \\ -e_{22} & e_{22} & 0 & e_{15} & 0 & 0 \\ e_{31} & e_{31} & e_{33} & 0 & 0 & 0 \end{pmatrix}$$

Stress Matrix

$$\varepsilon = \begin{pmatrix} \varepsilon_{11} & 0 & 0 \\ 0 & \varepsilon_{11} & 0 \\ 0 & 0 & \varepsilon_{33} \end{pmatrix}$$

Relative Permittivity Matrix

- **The elasticity matrix for an isotropic material such as gold and PMMA is shown in the following expression. Here, permittivity matrix will have all constants for the principal diagonal elements and the piezoelectric coupling matrix will be zero.**

$$C^E = E/(1+\nu)(1-2\nu) \begin{pmatrix} 1-\nu & \nu & \nu & 0 & 0 & 0 \\ \nu & 1-\nu & \nu & 0 & 0 & 0 \\ \nu & \nu & 1-\nu & 0 & 0 & 0 \\ 0 & 0 & 0 & 1-2\nu & 0 & 0 \\ 0 & 0 & 0 & 0 & 1-2\nu & 0 \\ 0 & 0 & 0 & 0 & 0 & 1-2\nu \end{pmatrix}$$

Elasticity Matrix

Where E is the Young's modulus and v is the Poisson ratio

Material Constants & Boundary Conditions

	Gold	PMMA
Density	1190 Kg/m^3	19300 Kg/m^3
Poisson Ratio	0.40	0.44
Young's Modulus	3 x 10^{9}Pa	70 x 10^9 Pa

XY Lithium Niobate *

c_{11}	20.3×10^{10} Nm^{-2}
c_{33}	24.5 ×10^{10} Nm^{-2}
c_{44}	6.0×10^{10} Nm^{-2}
c_{12}	5.3×10^{10} Nm^{-2}
c_{13}	7.5×10^{10} Nm^{-2}
c_{14}	0.9×10^{10} Nm^{-2}
e_{15}	3.7 Cm^{-2}
e_{22}	2.5 Cm^{-2}
e_{31}	0.2 Cm^{-2}
e_{33}	1.3 Cm^{-2}
ε_{11}	44
ε_{33}	29
ρ	4600 Kg m^{-3}

Electrical boundary conditions

Boundary	Electrical Condition
Top boundary of piezoelectric substrate	Zero charge/symmetry
Symmetric plane of piezoelectric substrate	Zero charge/symmetry
All other boundaries of the piezoelectric substrate	Ground
Alternate fingers of generator IDT	Scalar expression for Input wave function
Other fingers of generator IDT	Ground
Alternate fingers of receiver IDT	Zero charge/symmetry
Other fingers of receiver IDT	Ground

*Ref: G. Xu, Direct finite element analysis of frequency response of a Y-Z Lithium Niobate SAW filter, Smart Materials Structures 9 (2000) 973-980.

Results & Discussion

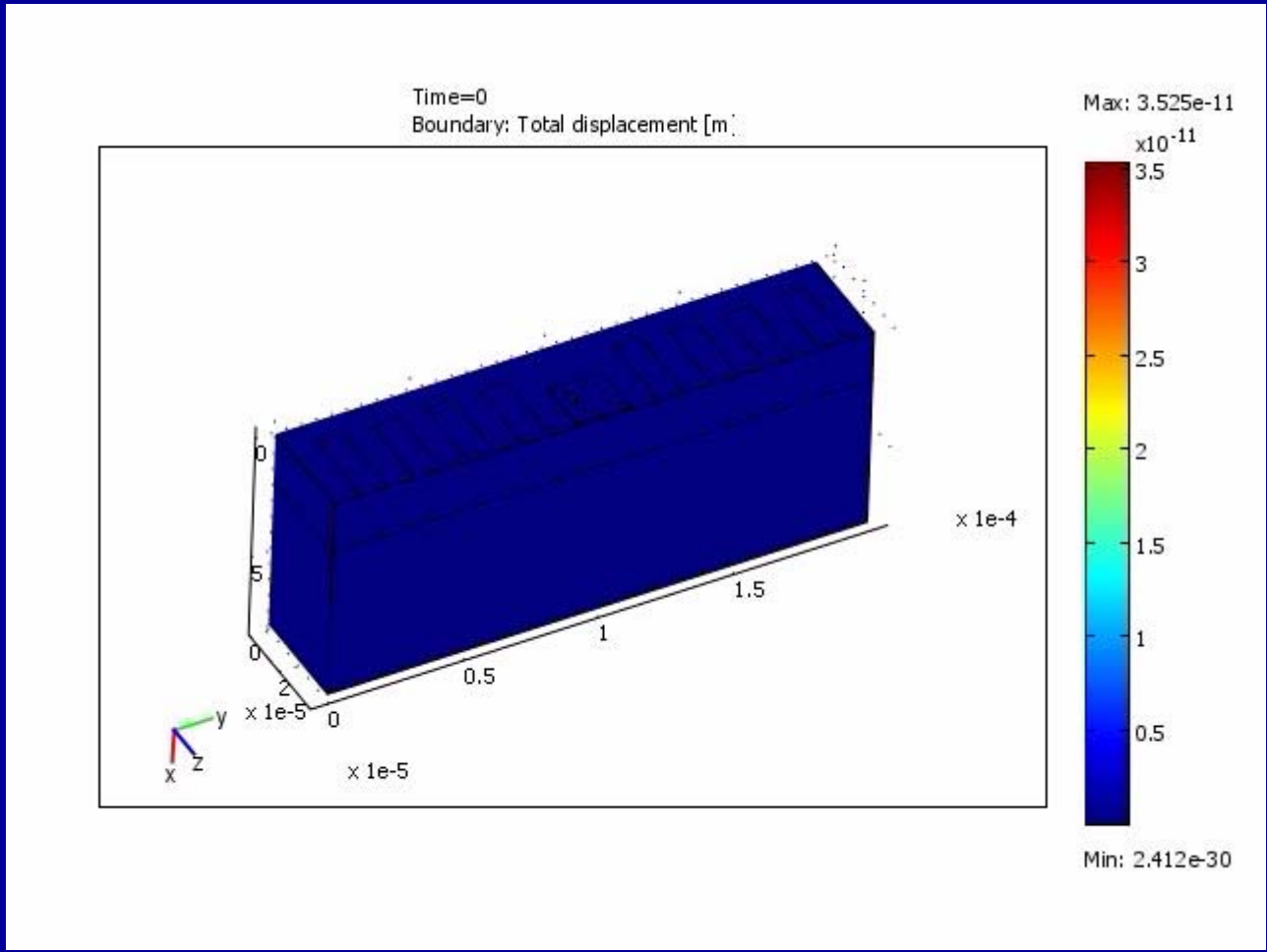

Animated file of total displacement of the 3-D SAW model with a thin film of gold coated on the piezoelectric substrate from 0 to 100nsec.

Results & Discussion

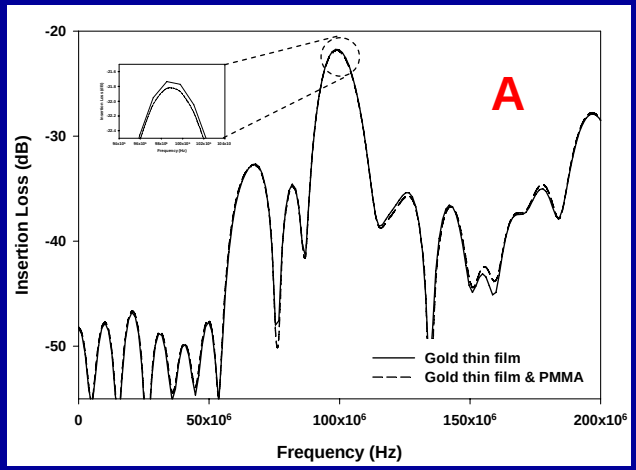

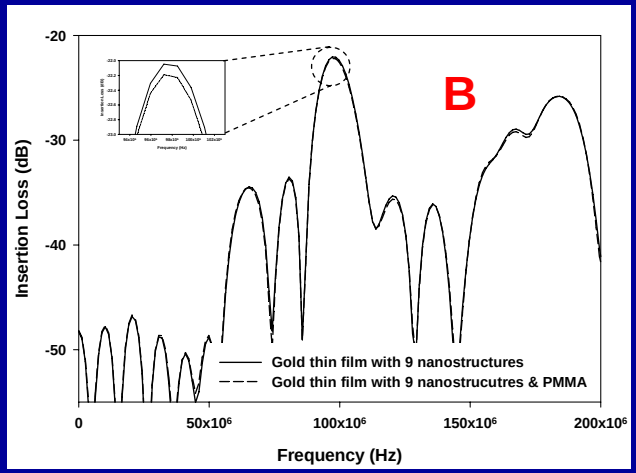

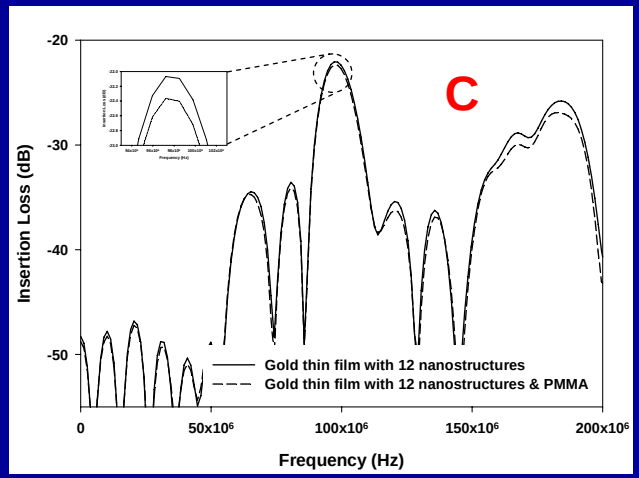

Insertion loss spectra in response to an impulse wave function for a SAW sensor with (A) a gold film as the active surface (B) a gold thin film and 9 nanopillars (C) a gold thin film and 12 nanopillars before and after PMMA adsorption. Inset: Zoom-in view of the peak frequency.

Results & Discussion

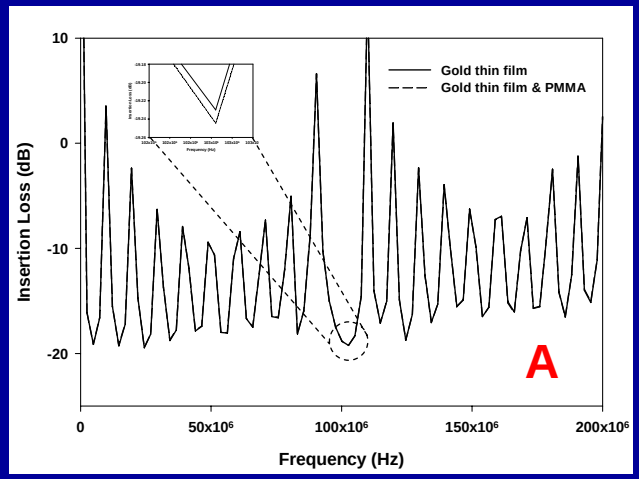

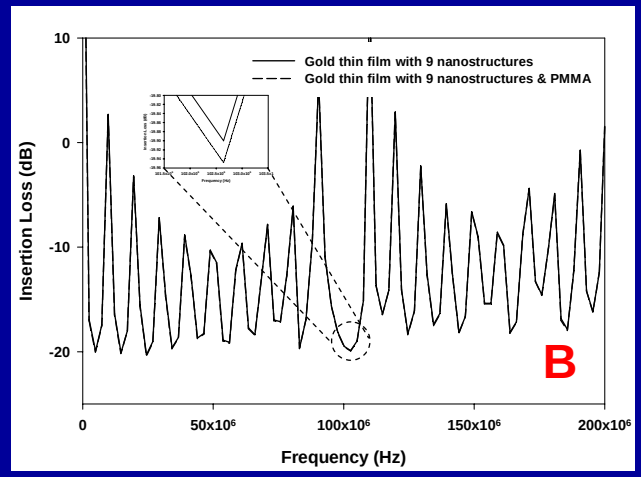

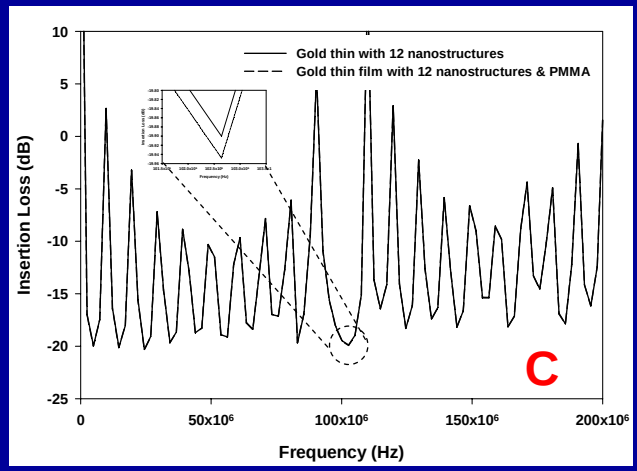

Insertion loss spectra in response to a sinusoidal wave function for a SAW sensor with (A) a gold film as the active surface (B) a gold thin film and 9 nanopillars (C) a gold thin film and 12 nanopillars before and after PMMA adsorption. Inset: Zoom-in view of the peak frequency.

Results & Discussion

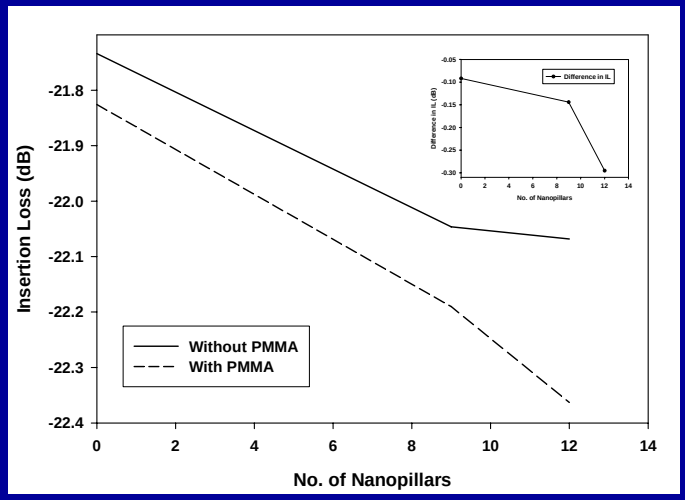

Amount of IL in SAW sensors with 0, 9 and 12 nanopillars in response to an impulse wave function before (as a baseline) and after PMMA adsorption. Inset: Difference in IL in reference to the baseline.

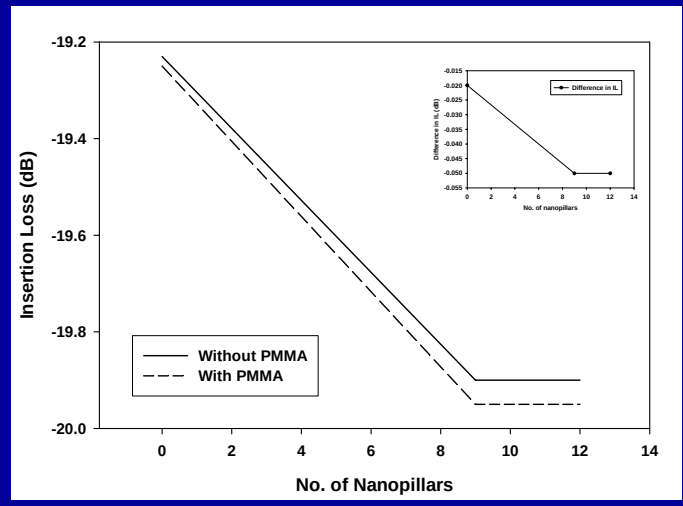

Amount of IL in SAW sensors with 0, 9 and 12 nanopillars in response to a sinusoidal wave function before (as a baseline) and after PMMA adsorption. Inset: Difference in IL in reference to the baseline.

Results & Discussion

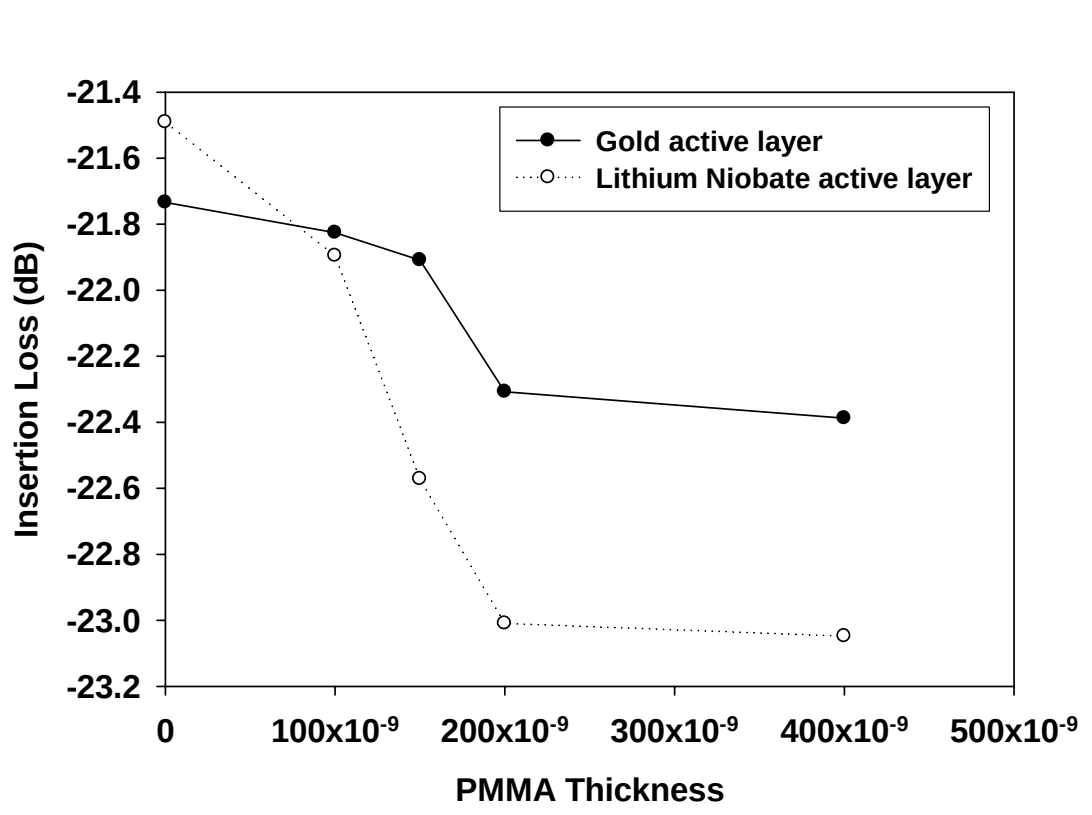

Variation of IL with the thickness of the adsorbed PMMA for a sensor with gold and lithium niobate as the active layer.

Conclusions

- Integration of nanopillars in the SAW sensors increases detection sensitivity.
- Detection sensitivity can be further increased by replacing the metallic active layer with a piezoelectric material.
- Impulse wave function perturbation is more effective in distinguishing small changes in mass loading than sinusoidal wave function perturbation.
- This work will help lay groundwork for developing new types of SAW sensors.

Acknowledgement

Thank you!

Acknowledgement
National Science Foundation
Institute of the Faculty of Engineering at The University of Georgia
College of Agricultural and Environmental Science at The University of Georgia